ORIGINAL SCIENTIFIC PAPER

CROATICA CHEMICA ACTA

*Croat. Chem. Acta* **2018**, *91*(1), 53–64
Published online: March 21, 2018
DOI: 10.5562/cca3289

HKD 1926

# Lignocellulosic Materials as Dye Adsorbents: Adsorption of Methylene Blue and Congo Red on Brewers' Spent Grain

Antonija Kezerle,[1] Natalija Velić,[2,*] Damir Hasenay,[3] Davor Kovačević[4]

[1] Vodovod-Osijek d.o.o., Poljski put 1, HR-31000, Osijek, Croatia
[2] Faculty of Food Technology Osijek, J. J. Strossmayer University of Osijek, F. Kuhača 20, HR-31000, Osijek, Croatia
[3] Faculty of Humanities and Social Sciences, J. J. Strossmayer University of Osijek, Lorenza Jägera 9, HR-31000, Osijek, Croatia
[4] Division of Physical Chemistry, Department of Chemistry, Faculty of Science, University of Zagreb, Horvatovac 102a, HR-10000, Zagreb, Croatia
* Corresponding author's e-mail address: natalija.velic@ptfos.hr

RECEIVED: January 20, 2018 ⋆ REVISED: March 12, 2018 ⋆ ACCEPTED: March 13, 2018

**Abstract:** Brewers' spent grain (BSG), a lignocellulosic waste material, was evaluated as a low-cost adsorbent for the removal of synthetic dyes methylene blue (MB) and Congo red (CR) from aqueous solutions in a batch process. Characterisation of the BSG was performed by chemical analysis, FTIR and SEM. The effects of contact time, initial dye concentration, adsorbent particle size, adsorbent concentration and pH on the adsorption process were investigated. High removal of both dyes ranging from 70 to over 90 % was achieved. It was shown that in both cases (MB and CR adsorption) the process could be interpreted in terms of Langmuir and Freundlich adsorption isotherms. The kinetics of the adsorption process was well described by the pseudo-second-order model. The results indicated the potential use of BSG as a low-cost adsorbent for MB and CR dye removal from aqueous solutions.

**Keywords**: adsorption, brewers' spent grain, Congo red, lignocellulose, methylene blue, synthetic dyes removal.

## INTRODUCTION

DYES are natural or synthetic compounds, usually organic in nature, that provide bright and lasting colour to other substance. They are extensively used in many industries such as textile, leather, paper, pharmaceutical, cosmetic, food and much more. Most commonly used dyes are synthetic by origin and often have complex aromatic molecular structure. To date, there are over 100000 different synthetic dyes available commercially.[1] Different industrial processes employing dyes are generators of a considerable amount of coloured wastewater. It has been reported that up to 1–10 % of dyes used can be lost to industrial effluents during the production process.[2] Apart from dyes, coloured wastewaters often contain other contaminants, *e.g.* textile wastewaters contain different salts that promote covalent bonding of dyes and fibres, as well as bases, acids and metals.[3] Furthermore, it is often essential to maintain pH value of textile dye bath using buffer systems.[4] Thus pH and ionic strength of coloured wastewaters are dependent on the production process. Synthetic dyes are distinguished by high stability to light, heat and oxidising agents; high solubility and recalcitrance towards biodegradation, which all leads to their prolonged persistence and bioaccumulation in the environment.[5,6] When wastewaters that are treated inadequately are discharged to surface waters, they significantly reduce the oxygen concentration and light penetration of recipient, thus detrimentally affecting the aquatic ecosystems.[5] Furthermore, many dyes pose toxicity (genotoxicity, mutagenicity and carcinogenicity) to aquatic organisms and can endanger human health *via* the food chain.[7,8,9] Low biodegradability of dyes significantly impairs their removal efficiency by conventional biological wastewater treatment methods.[10] The conventional methods employed for dye removal from wastewater are numerous. To name but few: adsorption, membrane separation, coagulation and flocculation, oxidation or ozonation.[11] However, adsorption is by

far the most often applied at industrial scale, due to its simplicity, versatility, efficiency and insensitivity to toxic pollutants.[12,13] The main drawback is the relatively high cost of conventional adsorbents, such as the most widely used activated carbon. To address this problem, various low-cost adsorbents have been extensively investigated for dye removal from wastewaters. By definition, the low-cost adsorbent is abundant in nature or is an industrial by-product or waste material that requires no or little processing.[12] Lignocellulosic waste materials arising from food and wood industry or agriculture represent a potential alternative to conventional adsorbents. Different adsorbents derived from industrial or agricultural wastes have been successfully used for dye removal from an aqueous solution such as apple pomace,[14,15] peanut hull,[1] sugar bagasse,[16,17] sugar beet waste,[15] barley husk,[18] brewers' spent grain,[19,20] wood sawdust,[15,21] fruit and vegetable peels,[22,11] *etc*. The main components of lignocellulosic materials responsible for adsorption are polymers: cellulose, hemicellulose and lignin, *i.e.* the adsorption is achieved through the interaction of dyes and functional groups of these polymers (*e.g.* –OH and –COOH). When used as biosorbents, lignocellulosic materials often undergo different modifications in order to improve their adsorption characteristics. Modifications include physical modifications (size reduction, heat treatment), chemical modifications (using acids, bases or organic solvents) and pyrolysis.[23] Brewers' spent grain (BSG) is brewery lignocellulosic waste material that accounts for 85 % of the total waste production in the brewery[24] and thus is widely available throughout the year. So far BSG was mostly used as feed or has been landfilled, and its exploitation as a valuable renewable resource has been neglected.[25] However, different investigations were conducted in order to evaluate BSG as an adsorbent for the removal of synthetic dyes, namely acid dyes – green, yellow, blue and orange 7,[20,26,27] Basic Blue 41, Reactive Black 5, and Acid Black 1,[28] malachite green,[15] methylene blue,[19] and Congo red.[29] Methylene blue (MB) is a cationic (basic) dye most commonly used for cotton, silk and leather dyeing.[30] The chemical structure of MB is given in Figure 1a. Apart from being used as a dye, MB also has many uses in medicine such as the use in diagnostic microbiology as a stain, treatment of hypotension, hypoxia, preoperative use in cardiac surgery, treatment of severe vasoplegia, use as antimalarial and more. It is considered a safe drug when used in therapeutic doses of less than 2 mg $kg^{-1}$.[31] Even though it is not strongly hazardous, it can cause various harmful effects in humans and animals, such as skin irritations, permanent eyes injuries, irritation of gastrointestinal tract – nausea, vomiting and diarrhoea, cyanosis, dyspnoea, convulsions and tachycardia.[30,31,32] Congo red (CR) is an anionic dye that belongs to azo class of dyes (Figure 1b), the most widely used class of dyes. It has been

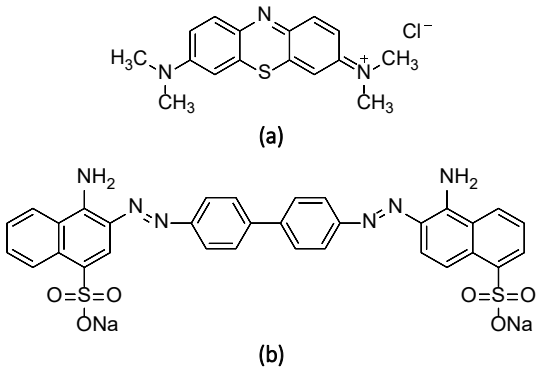


**Figure 1.** Chemical structures of MB (a) and CR (b).

extensively used in textile, paper, plastic and rubber industries. Furthermore, it has been used in microbiology for staining and for diagnostic purposes for staining amyloid in tissues of patients. CR proved to be toxic to many organisms and is suspected to be carcinogenic and mutagenic. Furthermore, it is hard to biodegrade due to its complex chemical structure.[33]

The aim of this study was to evaluate the potential of BSG as a low-cost adsorbent for the removal of synthetic dyes from buffered aqueous solutions. Widely used cationic dye MB and anionic azo dye CR were used as model dyes. Different factors influencing the adsorptive dye removal were investigated in order to find the optimum conditions for the efficient adsorption of dyes onto BSG: initial dye concentration, contact time, adsorbent size, adsorbent concentration and solution pH. This study provides the insight into potential application of widely available waste material BSG for adsorptive dye removal from aqueous solutions.

# EXPERIMENTAL

## Adsorbent

BSG was kindly donated by brewery "Osječka pivovara d.d.", Osijek, Croatia. Within few hours of collection from the mash tun BSG was spread on trays and oven dried at 60 °C for 48 h, to prevent microbial spoilage. Dried BSG (8 % moisture) was ground using standard laboratory knife mill with 1 mm screen (MF10 basic, IKA Labortechnik, Germany) and passed through the set of sieves mesh sizes 500, 400, 300, 200, 100 and 53 μm using a vibratory sieve shaker (AS 200 Digit, Retsch GmbH, Germany). The mass of BSG retained on each sieve was measured and the percentage of the total mass of the BSG sample was calculated. No other chemical or physical treatments were applied prior to adsorption experiments.

## Adsorbent Characterisation

The moisture content of dried BSG was determined

thermogravimetrically using moisture analyser (HR73 Moisture Analyser, Mettler Toledo, Switzerland). The determination of ash content and extractives was described elsewhere.[34] Protein content was determined using the Kjeldahl method. Lignin and cellulose contents were determined according to the procedures described elsewhere.[35,36] The surface functional groups of BSG affecting the adsorption were detected by Fourier transforms infrared (FTIR) spectrometer (Cary 630, Agilent Technologies). The spectra were recorded from 4000 to 400 $cm^{-1}$. BSG morphology and surface characteristics were studied using field emission scanning electron microscope (FE SEM, JOEL, JSM-7000F).

## Adsorbates

MB and CR used in this study were purchased from Merck and Fischer Scientific, respectively. Dried BSG added to MB and CR aqueous dye solutions yielded pH lower than 5. Thus it was decided to dissolve the dyes in buffer pH = 7, obtaining the solutions that partially simulate coloured industrial effluents. A stock solution of 500 mg $dm^{-3}$ of individual dyes was prepared by dissolving the exact quantity of dye in previously prepared pH = 7 buffer solution (0.025 mol $dm^{-3}$ $Na_2HPO_4$ / 0.025 mol $dm^{-3}$ $KH_2PO_4$). The experimental solutions were obtained by diluting the stock solution with buffer to the desired dye concentration.

## Batch Adsorption Studies

A batch technique was used for the investigation of MB and CR adsorption on BSG. A fixed amount of BSG (1 g) was added to a series of 250 $cm^3$ conical flasks containing 100 $cm^3$ of dye solutions of different initial concentrations (15–150 mg $dm^{-3}$) at constant pH. The flasks were placed in the incubator shaker (INNOVA 4340, New Brunswick Scientific, New Jersey, USA) at 298.15 K and 150 rpm for 240 min, to ensure equilibrium was reached. Flasks were collected from the incubator at predetermined time intervals for spectrophotometric determination of colour removal. The samples were filtered through Whatman filter paper No. 42 and then centrifuged at 10000 rpm for 5 min (Tehtnica Centric 322A, Domel d.o.o., Slovenia). The dye concentrations in clarified supernatants were determined immediately using spectrophotometer (Lambda 25, Perkin Elmer, USA) at appropriate wavelengths (MB 664 nm and CR 498 nm). The percent of dye removal was calculated by the following equation:

$$\%\ \text{dye removal} = \frac{\gamma_0 - \gamma}{\gamma_0} \cdot 100 \qquad (1)$$

where $\gamma_0$ and $\gamma$ (in mg $dm^{-3}$) are the initial dye concentration and dye concentration after predetermined contact time, respectively.

The amount of dye adsorbed at equilibrium onto BSG, $q_e$ (in mg $g^{-1}$), was calculated as follows:

$$q_e = \frac{(\gamma_0 - \gamma_e) \cdot V}{m} \qquad (2)$$

where $\gamma_e$ is the dye concentration at equilibrium (in mg $dm^{-3}$), $V$ is the dye solution volume (in $dm^3$) and $m$ is the mass of adsorbent used (in g).

To study the effect of BSG particle size on the amount of dye adsorption, three particle size ranges (53–100 μm, 100–400 μm and 400–500 μm) were used while keeping all the other parameters constant ($\gamma_{dye}$ = 30 mg $dm^{-3}$, $m_{adsorbent}$ = 1 g, $V_{dye\ solution}$ = 100 $cm^3$, pH = 6.8, $t$ = 240 min, $T$ = 298.15 K, 150 rpm). The effect of BSG concentration on the amount of dye adsorbed was studied by adding different amounts of BSG (0.5, 1.0 and 1.5 g) to a definite volume of dye solution ($V$ = 100 $cm^3$) and keeping all other parameters constant ($\gamma_{dye}$ = 30 mg $dm^{-3}$, pH = 6.8, $t$ = 240 min, $T$ = 298.15 K, 150 rpm).

To study the effect of solution pH on dye adsorption on BSG, 30 mg $dm^{-3}$ dye solution was prepared in a series of different buffers as follows: pH = 4 (0.05 mol $dm^{-3}$ potassium hydrogen phthalate, $C_8H_5KO_4$), pH = 6 (0.1 mol $dm^{-3}$ $C_8H_5KO_4$ / 0.1 mol $dm^{-3}$ NaOH), pH = 8 (0.2 mol $dm^{-3}$ $H_3BO_3$ / 1 mol $dm^{-3}$ NaOH / 0.1 mol $dm^{-3}$ HCl), pH = 9 (0.2 mol $dm^{-3}$ $H_3BO_3$ /1 mol $dm^{-3}$ NaOH / 0.1 mol $dm^{-3}$ HCl), and pH = 10 (0.025 mol $dm^{-3}$ $Na_2CO_3$ / 0.025 mol $dm^{-3}$ $NaHCO_3$).

The linear forms of Langmuir and Freundlich adsorption models were employed in describing the adsorption process. The kinetics of MB and CR adsorption were analysed by fitting the data to pseudo-first-order, pseudo-second-order and intraparticle diffusion models.

All the above-described experiments were performed in duplicate and were found reproducible.

# RESULTS AND DISCUSSION

## Adsorbent Characterization

To assess the chemical composition of BSG, a series of analysis was performed and the results are given in Table 1. As can be seen from the table, the lignocellulosic polymers lignin and cellulose comprise over 45 % of BSG's dry weight, while proteins account for another 21 %. The obtained results are consistent with the results of other studies reviewed by Mussato *et al.*[24] However, it is important to note that BSG's chemical composition can considerably vary between different breweries, due to variation in technology or differences in malt used during brewing.[37]

To investigate the qualitative adsorption characteristics of BSG's surface functional groups, FTIR spectra were recorded and the results are presented in Figure 2. The spectra revealed a number of adsorption peaks, indicating

**Table 1.** Chemical composition of BSG

| Compound | % dry weight |
|---|---|
| Ash | 3.5 |
| Extractives[a] | 10.2 |
| Total lignin | 23.6 |
| *Klason lignin* | 14.5 |
| *Acid soluble lignin* | 9.1 |
| Cellulose | 22.0 |
| Proteins | 21.0 |
| Undetermined | 19.7 |

[a] ethanol/benzene (1:1)

the complex nature of the BSG. FTIR spectrum of BSG is dominated by the broad bands at 3280 $cm^{-1}$ representing hydroxyl groups (–OH). The bands are attributed to O–H stretching vibrations due to inter and intramolecular hydrogen bonding of polymeric compounds, such as cellulose and lignin, indicating the presence of free hydroxyl groups at the adsorbent surface. The bands with two maxima at 2922 and 2855 $cm^{-1}$ could be ascribed to aliphatic (–CH) groups stretching. In the 2000–400 $cm^{-1}$ region, the spectrum is dominated by the intense band at 1036 $cm^{-1}$ probably arising from the polysaccharides, *i.e.* it could be assigned to C–O, C=C and C–C–O stretching in cellulose, hemicellulose and lignin. Furthermore, the band observed at 1625 $cm^{-1}$ could be assigned to a carbonyl group (C=O) of unionised carboxylate stretching of carboxylic acid, while the peak at 1535 $cm^{-1}$ could be assigned to aromatic ring vibration from lignin. The band at 521 $cm^{-1}$ could be ascribed to ester vibrations and monosubstituted aromatic rings of the lignin fraction. The shifting of peak positions, *i.e.* the change in the frequency of peaks and intensity of peaks of dye-loaded BSG samples compared to that of BSG that can be observed from the spectra, indicate the adsorption of dyes at the surface of BSG.

In order to study the surface morphology of BSG, the most commonly used characterization technique, *i.e.* scanning electronic microscopy (SEM), was employed. The surface morphology of BSG at 1000, 2000, 5000 and 10000 magnifications is shown in Figure 3. The figures revealed the irregular shape of BSG particles, as well as a rough surface containing micropores, that may provide substantial adsorption surface for dyes.

## Batch Adsorption Studies

### Effect of Initial Dye Concentration and Contact Time on Dye Adsorption

The contact time between the adsorbent and the dye has a strong effect on the adsorption process. Figure 4 shows the effect of the initial dye concentration and contact time on MB and CR adsorption to BSG. The adsorption increased with the increase of contact time and the increase of initial dye concentration. The amount of MB removed at equilibrium increased from 1.35 to 12.8 mg $g^{-1}$, while the amount of removed CR increased from 1.41 to 13.21 mg $g^{-1}$ when the initial dye concentration increased from 15 to 150 mg

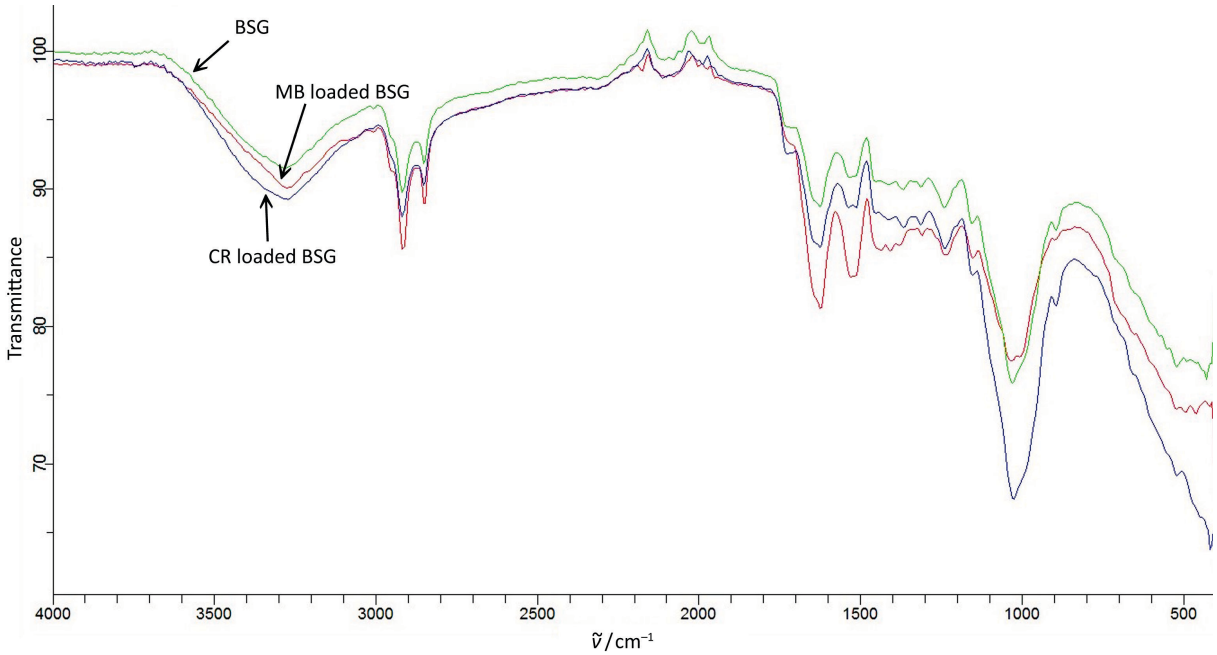


**Figure 2.** The FTIR spectral characteristics of BSG before and after MB and CR adsorption.

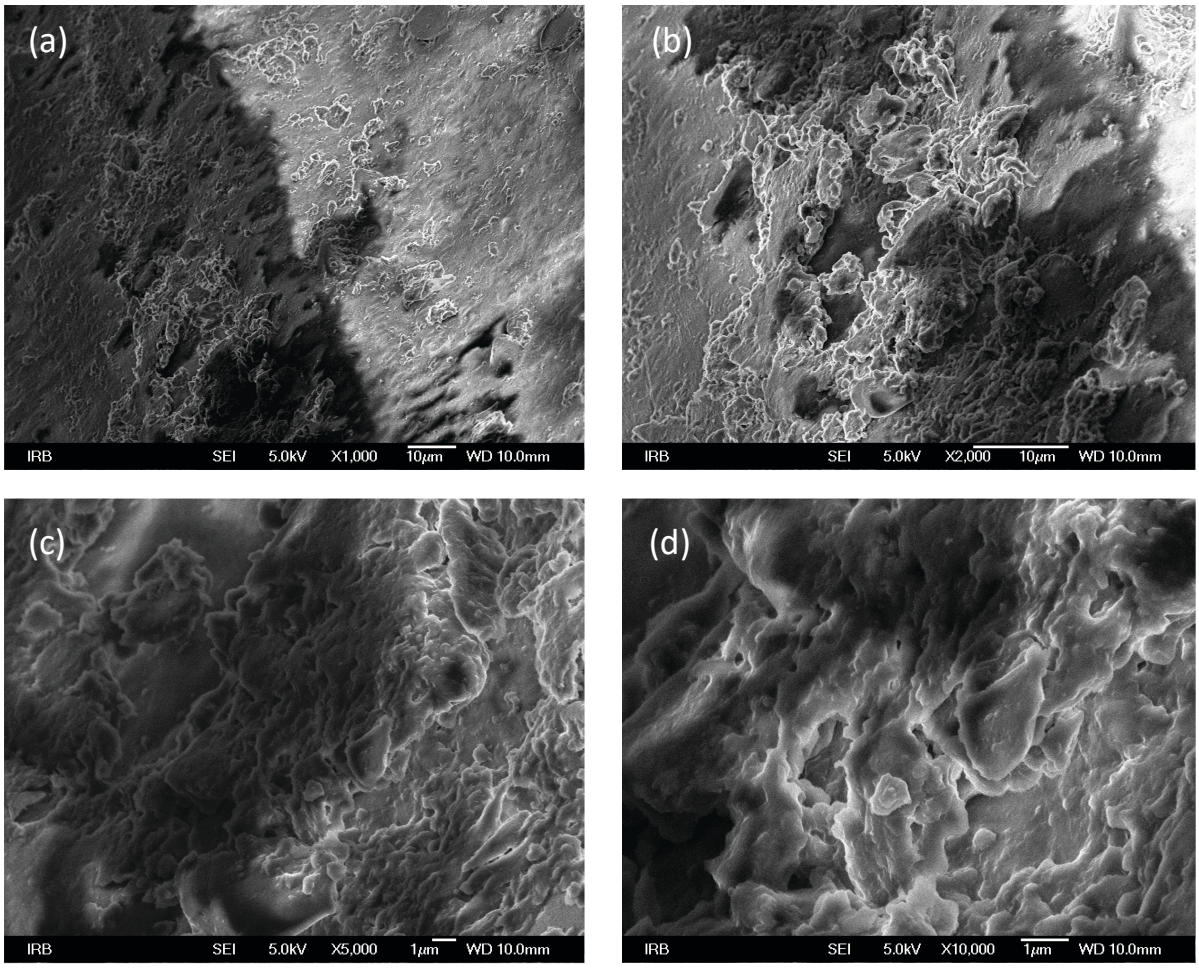


**Figure 3.** SEM micrograph of BSG at different magnifications: 1000 (a), 2000 (b), 5000 (c), 10000 (d).

$dm^{-3}$. These results indicated that the MB and CR adsorptive removal using BSG is dependent on the concentration of dye and are consistent with those of other studies using different biosorbents for MB and CR removal, such as garlic peel,[11] jackfruit peel,[38] neem sawdust,[39] roots of *Eichhornia crassipes*,[40] and waste banana pith.[41] Higher initial concentration results in a higher concentration gradient, thus providing the higher driving force to overcome the resistance to the dye mass transfer between the two phases – the aqueous and solid. Consequently, the amount of dye adsorbed at equilibrium increased.[42] Table 2 gives a shortened overview of the effect of contact time and initial dye concentration on the percentage of dye removal. Removal of both dyes is characterised by rapid removal during the first 20 min of the experiment. After the initial rapid dye removal, at later stages, the removal becomes slower until equilibrium is achieved. The higher removal rate at the initial stages of the adsorption process can be attributed to the larger unoccupied surface area available for dye adsorption, while at later stages there are fewer remaining unoccupied surface sites and the removal rate becomes slower.[40] The adsorption removal of both dyes was characterised by a high percentage of dye removal (85–96 %) independent of the applied dye concentration.

### Effect of Adsorbent Particle Size and Concentration on Dye Adsorption

The effect of particle size on the adsorption of MB and CR onto BSG is shown in Figure 5. Three particle size ranges were selected based on the results of the milled BSG particle size determination by sieve analysis (data not shown), namely 53–100 μm, 100–400 μm and 400–500 μm. 97 % of all BSG particles were distributed among the ranges mentioned above. The sieve analysis results revealed that the highest percentage of the total mass of the BSG sample used for the analysis (68 %) were particles ranging from 100 to 400 μm. In respect to the possible application of BSG for dye removal at industrial scale, it is important to choose the particle size range that will ensure the least possible amount of discarded adsorbent material, while keeping the

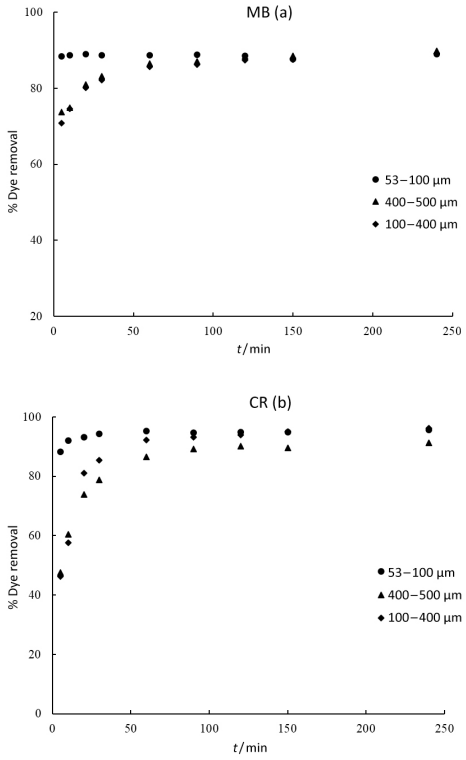


**Figure 5.** The effect of particle size on the adsorption of MB (a), and CR (b) onto BSG. $\gamma_{dye}$ = 30 mg dm$^{-3}$, $t$ = 240 min, $T$ = 298.15 K, $m_{adsorbent}$ = 1 g, $V_{dye\ solution}$ = 100 cm$^3$, pH = 6.8.

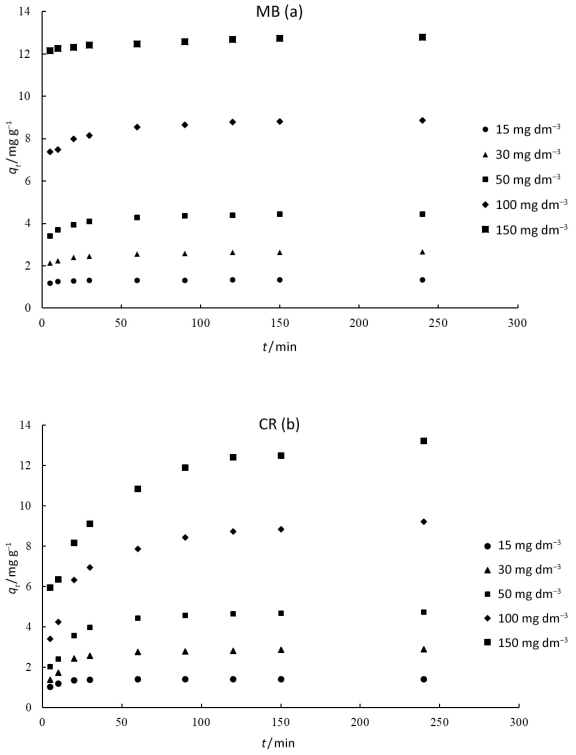


**Figure 4.** The effect of the initial dye concentration and contact time on MB adsorption (a), and CR adsorption (b). $T$= 298.15 K, $m_{adsorbent}$ = 1 g, $V_{dye\ solution}$ = 100 cm$^3$, pH = 6.8.

high removal percentage. As can be seen from the Figure 5 the effect of particle size is evident during the first 50 min of the experiment, *i.e.* the amount of dye adsorbed increased as the particle size of the adsorbent decreased. This can probably be attributed to the fact that smaller particles provide a larger external surface area per unit mass, thus removing more dye at the initial stages of the experiment.[39] At later stages of the experiment, the effect of particle size on dye adsorption was not prominent. The adsorption is usually strongly affected by the adsorbent concentration, because of the surface area available for adsorption. The effect of adsorbent concentration on the percentage removal of MB and CR is presented in Figure 6. Both MB and CR percentage removal increased with the increase of adsorbent concentration, which was explicitly evident during the initial stages of the adsorption process. This is in agreement with the report of the MB adsorption on *Oleander* plant tissues,[43] as well as the adsorption of CR onto *E. crassipes* roots.[40]

### Effect of Solution pH on Dye Adsorption

Generally, pH is an important factor affecting the adsorptive removal of different contaminants from waste–water.[42] The effect of solution pH on the amount of dye

**Table 2.** The effect of contact time and initial dye concentration on MB and CR removal by BSG. $T$= 298.15 K, $m_{adsorbent}$ = 1 g, $V_{dye\ solution}$ = 100 cm$^3$, pH = 6.8

| Dye | $t$ / min | Initial dye concentration / mg dm$^{-3}$ | | | | |
|---|---|---|---|---|---|---|
| | | 15 | 30 | 50 | 100 | 150 |
| | | Dye removal / % | | | | |
| MB | 20 | 85.73 | 80.10 | 78.82 | 79.91 | 82.13 |
| | 240 | 89.87 | 89.10 | 88.89 | 88.57 | 85.33 |
| CR | 20 | 89.00 | 81.04 | 71.33 | 69.47 | 60.73 |
| | 240 | 93.43 | 96.19 | 94.72 | 92.15 | 88.04 |

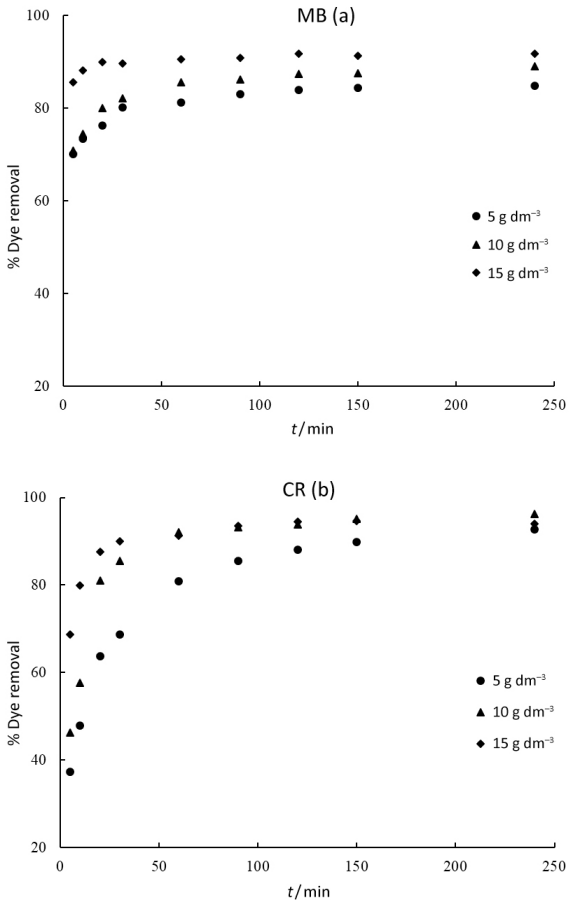


**Figure 6.** The effect of adsorbent concentration on the adsorption of MB (a), and CR (b) onto BSG. $\gamma_{dye}$ = 30 mg dm$^{-3}$, $t$ = 240 min, $T$ = 298.15 K, pH = 6.8.

adsorbed on BSG at equilibrium was investigated for MB and CR dissolved in a series of different buffers over the pH range of 4–10. The results are presented in Figure 7 show that the amount of MB adsorbed was minimal at pH = 4, increased with pH up to pH = 8 and then remained constant over the pH range 8–10. This is in agreement with the study of adsorptive MB removal using garlic peel[11] that also reported constant dye adsorption over the pH range 6–12 and lower adsorption at acidic pH. The unfavourable effect of low pH on MB removal was also reported by other studies using different adsorbents, such as cedar sawdust,[44] spent mushroom substrate,[45] jackfruit peel,[38] cellolignin – a wood industry by-product,[46] *etc*. Less efficient MB removal at low pH can probably be attributed to the presence of positively charged $H^+$ ions that compete with MB cations for adsorption sites. The amount of CR adsorbed was minimal at pH = 4, increased up to pH = 7 and then decreased over the pH range 8–10. These results differ from the published study that reported the maximum CR adsorption at pH = 5 and constant percentage of removal

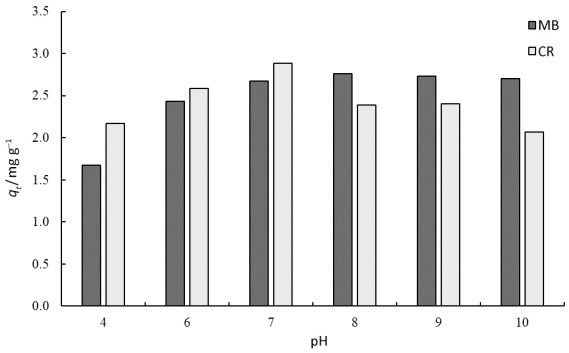


**Figure 7.** The effect of pH on the adsorption of MB and CR onto BSG. $\gamma_{dye}$ = 30 mg dm$^{-3}$, $t$ = 240 min, $T$ = 298.15 K, $m_{adsorbent}$ = 1 g, $V_{dye\ solution}$ = 100 cm$^3$, pH = 6.8.

over pH range of 5.5–10.0 when cattail root was used as an adsorbent.[47] Furthermore, the study that used waste banana pith as adsorbent reported 92 % CR removal in the pH range 2–11,[41] while the study that used cassava residue also reported that pH did not markedly affect the adsorptive capacity.[48] The discrepancy in the results between our study and the studies mentioned above may be attributed to the fact that buffered aqueous CR solution was used in our study. Even though buffers could interfere with the dye adsorption to some extent,[4] the removal efficiencies of both MB and CR in this study were in the range of 70–90 % over the entire pH range from 4 to 10, regardless the used buffer.

## Adsorption Equilibrium

The adsorption isotherm describes how the adsorbate molecules distribute between the liquid and solid phase at the adsorption equilibrium, and offers some insight of the adsorption capacity of the adsorbent.[11] The adsorption data were fitted to the Langmuir and Freundlich equations.

### Langmuir Isotherm

Langmuir isotherm model presumes the occurrence of adsorption at specific adsorbent homogenous sites as a monolayer. Furthermore, the model assumes the availability of a fixed number of adsorption sites and the reversible nature of adsorption.[49] The linear form of Langmuir isotherm[50] equation used is represented by the following equation:

$$\frac{\gamma_e}{q_e} = \frac{1}{q_m} \cdot \gamma_e + \frac{1}{K_L \cdot q_m} \tag{3}$$

where $\gamma_e$ (in mg dm$^{-3}$) is the equilibrium concentration, $q_e$ (mg g$^{-1}$) is the amount of dye adsorbed per unit mass of adsorbate, $q_m$ (in mg g$^{-1}$) is the maximum amount of dye adsorbed (monolayer adsorption capacity) and $K_L$ (dm$^3$ mg$^{-1}$) is the Langmuir constant related to the free energy of adsorption. Both $q_m$ and $K_L$ can be predicted from the plot

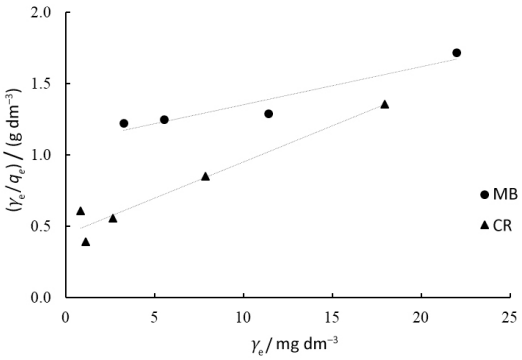


**Figure 8.** Langmuir isotherm of MB and CR adsorption on BSG at 298.15 K.

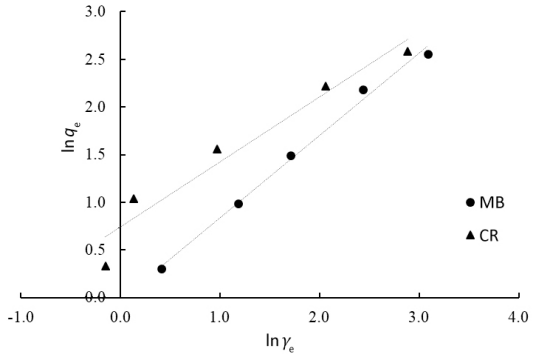


**Figure 9.** Freundlich isotherm of MB and CR adsorption on BSG at 298.15 K.

of $\gamma_e/q_e$ against $\gamma_e$ (Figure 8). The Langmuir isotherm parameters obtained in this study are given in Table 3. The dimensionless constant called equilibrium parameter $R_L$ represents the essential characteristics of the Langmuir isotherm and can be calculated by the following equation:

$$R_L = \frac{1}{1 + K_L \cdot \gamma_0} \tag{4}$$

Where $\gamma_o$ (in mg dm$^{-3}$) is the highest initial dye concentration. The $R_L$ values indicate the type of isotherm to be unfavourable ($R_L$ >1), favourable (0 < $R_L$ < 1), linear ($R_L$ = 1) or irreversible ($R_L$ = 0).[16] The $R_L$ values in this study were 0.214 and 0.055 for MB and CR, respectively, confirming that MB and CR adsorption onto BSG under studied conditions was a favourable process. However, when experimentally obtained $q_{m\,exp}$ values were compared to the $q_{m\,cal}$ values calculated on the basis of Eq. 3, the comparison revealed that CR equilibrium data were in better accordance with Langmuir isotherm equation than MB data.

However, it should be taken into account that the basic assumptions of classical Langmuir equation are not easily met under real experimental conditions since the deviation of a real adsorption system from the ideal one was not accounted in the derivation process of the classical Langmuir equation.

### Freundlich Isotherm

The Freundlich isotherm model describes the non-ideal adsorption on heterogeneous surfaces and multilayer adsorption, with no uniform distribution of adsorption heat. The linear form of the Freundlich equation[51] can be expressed as:

$$\ln q_e = \ln K_F + \frac{1}{n} \cdot \ln \gamma_e \tag{5}$$

where $q_e$ (in mg g$^{-1}$) is the amount of dye adsorbed at equilibrium and $\gamma_e$ (in mg dm$^{-3}$) is the equilibrium concentration of dye in solution. $K_F$ and $n$ are Freundlich isotherm constants indicating the adsorbent adsorption capacity ($K_F$) and the favourability of the adsorption process ($n$). The calculated Freundlich constants are also given in Table 3. The values of $n$ give the measure of deviation from linearity of the adsorption, and it has been proposed that $n$ = 1 means that adsorption is linear, $n$ < 1 indicates that adsorption is a chemical process, while $n$ > 1 indicates favourable adsorption achieved by the physical process.[16] The results presented in Figure 9 and Table 3 (Freundlich isotherm parameters) indicate that the adsorption of MB and CR onto BSG is favourable and experimental data can be described by the Freundlich model.

## Adsorption Kinetics

Generally, adsorption kinetics could be analysed by means of various linear[52,53] and non-linear[54] forms of models. Here, the experimental kinetics data of MB and CR adsorption onto BSG were fitted using three selected models: linear pseudo-first-order and pseudo-second-order models and intraparticle diffusion kinetic model. The summarised kinetic parameters of the pseudo-first-order and pseudo-second-order models and linear plots of intraparticle diffusion kinetic model are shown in Tables 4 and 5 and Figure 10, respectively.

### Pseudo-first-order and Pseudo-second-order Models

One of the most widely used adsorption rate equations applicable for the liquid/solid system adsorption based on the adsorbent (solid) capacity is the Lagergren[52] equation represented as follows:

$$\ln(q_e - q_t) = \ln q_e - k_1 t \tag{6}$$

where $q_e$ and $q_t$ (in mg g$^{-1}$) are the amounts of dye adsorbed at equilibrium and at time $t$ (in min), respectively. $k_1$ (in min$^{-1}$) is the pseudo-first-order adsorption rate constant. The adsorption rate constant $k_1$ and $q_e$ were calculated from the plots of $\ln(q_e - q_t)$ *vs.* $t$ for different initial concentrations of MB and CR. This model assumes that the rate of adsorption is proportional to the number of the sites unoccupied by the solutes.[55]

**Table 3.** Isotherm parameters for the removal of MB and CR by BSG at 298.15 K

| Isotherm model and parameters | | MB | CR |
|---|---|---|---|
| Langmuir | $q_{m\,exp.}$ / mg g$^{-1}$ | 12.800 | 13.206 |
| | $q_{m\,cal.}$ / mg g$^{-1}$ | 37.45 | 19.65 |
| | $K_L$ / dm$^3$ mg$^{-1}$ | 0.025 | 0.114 |
| | $R_L$ | 0.213 | 0.055 |
| | $R^2$ | 0.929 | 0.953 |
| Freundlich | $K_F$ / (mg/g (dm$^3$/mg)$^{1/n}$) | 0.973 | 2.090 |
| | $n$ | 1.16 | 1.46 |
| | $R^2$ | 0.993 | 0.944 |

The data were further analysed by pseudo-second-order chemisorption model proposed by Ho and McKay[53] and expressed by the equation:

$$\frac{1}{q_t} - \frac{1}{q_e} = \frac{1}{k_2 \cdot q_e^2 \cdot t} \quad (7)$$

where $k_2$ (in g mg$^{-1}$ min$^{-1}$) is the pseudo-second-order rate constant of the adsorption process. The values of $q_e$ and $k_2$ were determined from the slope and intercept of the plot of $t$ / $q_t$ against $t$ for different initial MB and CR concentrations and the straight lines were obtained in all cases. The pseudo-second-order model assumes that the rate-limiting step that controls the adsorption might be chemisorption, *i.e.* chemical reactions.[56]

The kinetic parameters of the pseudo-first-order and pseudo-second-order models are summarised in Table 4. The goodness of fit was based on the correlation coefficient ($R^2$) values obtained for each model and each initial concentration of MB and CR. As can be seen from Table 4, the pseudo-second-order model appears to be better fitting than the pseudo-first-order model. Furthermore, although the $R^2$ values of pseudo-first-order model were relatively high, the calculated $q_{e\,cal}$ values are not in a good agreement with the experimental $q_{e\,exp}$ values. On the other hand, the $q_{e\,cal}$ values calculated using the pseudo-second-order model were very close to the experimental $q_{e\,exp}$ values. This indicates that pseudo-second-order model better describes the experimental kinetics data for both dyes, which is in a good agreement with other studies dealing both with MB[11,38,44,45] and CR.[40,48,57]

### Intraparticle Diffusion Model

Since pseudo-first-order and pseudo-second-order models cannot be used to describe the diffusion mechanism, Weber and Morris[58] proposed the intraparticle diffusion model. The equation below is used to evaluate the effect of intraparticle diffusion resistance on adsorption:

$$q_t = k_i \cdot t^{\frac{1}{2}} + C \quad (8)$$

where $k_i$ (in mg g$^{-1}$ min$^{-0.5}$) is the intraparticle diffusion rate constant, while $C$ is providing the information regarding the boundary layer thickness (larger intercept value indicates the greater boundary layer effect). The plots of $q$ *vs.* $t^{1/2}$ for different initial MB and CR concentrations are given in Figure 10, while the parameters of the intraparticle kinetic model are given in Table 5. If the plots pass through the origin, the intraparticle diffusion is the only rate-limiting step. However, if not (*i.e.* $C \neq 0$), the adsorption is to some extent also controlled by the boundary layer diffusion.[59] The plots for both MB and CR did not pass through the origin (Figure 10, Table 5), indicating that intraparticle diffusion was not the only process that controlled the adsorption of MB and CR onto BSG. The intercepts $C$ are

**Table 4.** Parameters of the pseudo-first-order and pseudo-second-order kinetic models for the removal of MB and CR by BSG at 298.15 K

| Dye | Pseudo-first-order kinetic | | | | | Pseudo-second-order kinetic | | |
|---|---|---|---|---|---|---|---|---|
| | $\gamma_0$ / mg dm$^{-3}$ | $q_{e\,exp}$ / mg g$^{-1}$ | $k_1$ / min$^{-1}$ | $q_{e\,cal}$ / mg g$^{-1}$ | $R^2$ | $k_2$ / g mg$^{-1}$ min$^{-1}$ | $q_{e\,cal.}$ / mg g$^{-1}$ | $R^2$ |
| MB | 15 | 1.348 | 0.013 | 0.094 | 0.791 | 0.626 | 1.348 | 0.999 |
| | 30 | 2.673 | 0.017 | 0.421 | 0.926 | 0.151 | 2.687 | 0.999 |
| | 50 | 4.445 | 0.025 | 1.561 | 0.984 | 0.093 | 4.488 | 1 |
| | 100 | 8.857 | 0.026 | 0.914 | 0.987 | 0.051 | 8.929 | 0.999 |
| | 150 | 12.800 | 0.015 | 0.677 | 0.975 | 0.083 | 12.821 | 1 |
| CR | 15 | 1.414 | 0.029 | 0.175 | 0.822 | 0.485 | 1.424 | 1 |
| | 30 | 2.886 | 0.024 | 0.966 | 0.906 | 0.065 | 2.951 | 0.999 |
| | 50 | 4.736 | 0.019 | 4.864 | 0.962 | 0.027 | 4.904 | 0.999 |
| | 100 | 9.215 | 0.026 | 2.159 | 0.951 | 0.009 | 9.597 | 0.999 |
| | 150 | 13.206 | 0.017 | 7.216 | 0.977 | 0.006 | 13.736 | 0.998 |

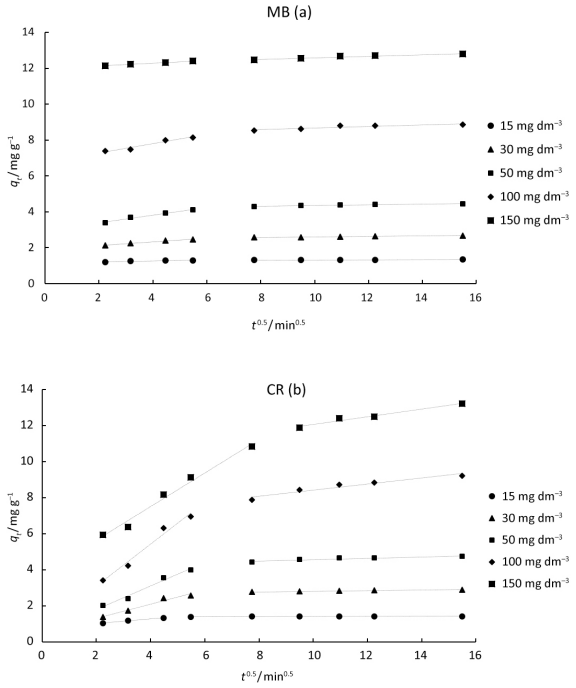


**Figure 10.** Weber and Morris intraparticle diffusion plots for MB (a), and CR (b) removal using BSG at different initial dye concentrations.

proportional to the thickness of the boundary layer and the examination of *C* values provides the information on the extent of thickness. Furthermore, higher values of *C* indicate higher adsorption capacities of adsorbent.[57] The plots in Figure 10 can be separated into two linear regions, indicating more than one mode of adsorption in the uptake of MB and CR by BSG. The first linear region can probably be assigned to the adsorption at the external adsorbent surface when the uptake rate is high. The second linear region can be attributed to the gradual adsorption stage and the equilibrium stage when the effect of the intraparticle diffusion is slowing down and ceasing. Similar results were reported for adsorption of MB on garlic peel and jackfruit peel,[11,38] as well as for adsorption of CR on cattail root.[47]

## CONCLUSION

Brewers' spent grain (BSG), a low-cost lignocellulosic material widely available throughout the year, was found to be effective for the removal of methylene blue (MB) and congo red (CR) from buffered aqueous solutions. High removal of both dyes ranging from 70 to over 90 % was achieved. The equilibrium data of both dyes were fitted to Langmuir and Freundlich isotherm models, and it was shown that in both cases (MB and CR adsorption) the process could be interpreted in terms of Langmuir and Freundlich adsorption isotherms. However, based on the $R^2$ values and the comparison of the calculated monolayer adsorption capacity ($q_{m\,cal}$) values and the experimental ($q_{m\,exp}$) values, the equilibrium data of CR seem to be somewhat better fitted with Langmuir isotherm equation than MB data. The kinetic data of the adsorption process for both MB and CR were well described by the pseudo-second-order kinetic model. When experimental kinetics data were fitted using intraparticle diffusion kinetic model the results indicated that intraparticle diffusion was not the only process that controlled the adsorption of MB and CR onto BSG. The results showed that BSG could be used as a low-cost adsorbent for the removal of synthetic dyes MB and CR from aqueous solutions, with a potential use for coloured wastewaters treatment. However, further research regarding different BSG modifications in order to improve its adsorption capacity is strongly recommended.

**Table 5.** Parameters of the intraparticle kinetic model for the removal of MB and CR by BSG at 298.15 K

| Dye | $\gamma_0$ / mg dm$^{-3}$ | $k_{i\,1}$ / mg g$^{-1}$ min$^{-0.5}$ | $C_1$ | $R_1^2$ | $k_{i\,1}$ / mg g$^{-1}$ min$^{-0.5}$ | $C_2$ | $R_2^2$ |
|---|---|---|---|---|---|---|---|
| MB | 15 | 0.0331 | 1.130 | 0.904 | 0.004 | 1.284 | 0.878 |
| | 30 | 0.107 | 1.897 | 0.983 | 0.014 | 2.461 | 0.973 |
| | 50 | 0.213 | 2.966 | 0.983 | 0.019 | 4.168 | 0.854 |
| | 100 | 0.261 | 6.751 | 0.959 | 0.041 | 8.275 | 0.830 |
| | 150 | 0.076 | 11.993 | 0.979 | 0.043 | 12.175 | 0.914 |
| CR | 15 | 0.132 | 0.750 | 0.991 | 0.003 | 1.369 | 0.754 |
| | 30 | 0.386 | 0.545 | 0.962 | 0.016 | 2.642 | 0.974 |
| | 50 | 0.645 | 0.515 | 0.978 | 0.037 | 4.194 | 0.893 |
| | 100 | 1.158 | 0.782 | 0.976 | 0.165 | 6.767 | 0.929 |
| | 150 | 0.931 | 3.780 | 0.983 | 0.210 | 9.963 | 0.969 |

## REFERENCES


[1] R. Gong, M. Li, C. Yang, Y. Sun, J. Chen, *J. Hazard. Mater.* **2005**, *121*, 247.

[2] Y. Wong, J. Yu, *Water Res.* **1999**, *33*, 3512.

[3] Arslan, I. A. Balcioglu, D. W. Bahnemann, *Appl. Catal. B Environ*. **2000**, *26*, 193.

[4] B. C. Burdett, C. C. Cook, J. Guthrie, *JSDC* **1977**, *93*, 55.

[5] M. S. M. Annuar, S. Adnan, S. Vikineswary, Y. Chisti, *Water*, *Air, Soil Pollut.* **2009**, *202*, 179.

[6] G. Crini, *Bioresour. Technol*. **2006**, *97*, 1061.

[7] N. Puvaneswari, J. Muthukrishnan, P. Gunasekaran, *Indian J. Exp. Biol.* **2006**, *44*, 618.

[8] N. Mathur, P. Bhatnagar, P. Bakre, *Appl. Ecol. Environ. Res.* **2006**, *4*, 111.

[9] G. B. Michaels, D. L. Lewis, *Environ. Toxicol. Chem.* **1985**, *4*, 45.

[10] O. Yesilada, D. Asma, S. Cing, *Process Biochem.* **2003**, *38*, 933.

[11] B. H. Hameed, A. A. Ahmad, *J. Hazard. Mater.* **2009**, *164*, 870.

[12] M. Rafatullah, O. Sulaiman, R. Hashim, A. Ahmad, *J. Hazard. Mater.* **2010**, *177*, 70.

[13] V. K. Gupta, Suhas, *J. Environ. Manage*. **2009**, *90*, 2313.

[14] T. Robinson, B. Chandran, P. Nigam, *Bioresour. Technol.* **2002**, *85*, 119.

[15] N. Velić, T. Marček, T. Jurić, K. Petrinović, D. Hasenay, L. Begović, V. Slačanac in *Proceedings of 15th Ružička days "Today science - tomorrow industry"* (Eds.: D. Šubarić, A. Jukić), J.J. Strossmayer University of Osijek, Faculty of Food Technology Osijek, Croatian Society of Chemical Engineers, Osijek and Zagreb, **2015**, pp. 424–432.

[16] S. Sadaf, H. N. Bhatti, S. Nausheen, S. Noreen, *Arch. Environ. Contam. Toxicol.* **2014**, *66*, 557.

[17] L. W. Low, T. T. Teng, A. Ahmad, N. Morad, Y. S. Wong, *Water, Air, Soil Pollut.* **2011**, *218*, 293.

[18] T. Robinson, B. Chandran, P. Nigam, *Water Res.* **2002**, *36*, 2824.

[19] A. Kezerle, T. Jurić, N. Velić, D. Hasenay, T. Marček, D. Velić in *Proceedings & abstracts of 9th International scientific/professional conference Agriculture in nature and environment protection* (Eds.: S. Rašić, P. Mijić), Glas Slavonije d.d., Osijek, **2016**, pp. 204–208.

[20] V. Jaikumar, *Int. J. Chem. (Toronto, ON, Can.)* **2007**, *1*, 2.

[21] V. Dulman, S. M. Cucu-Man, *J. Hazard. Mater.* **2009**, *162*, 1457.

[22] G. Annadurai, R. S. Juang, D. J. Lee, *J. Hazard. Mater*. **2002**, *92*, 263.

[23] A. Abdolali, W. S. Guo, H. H. Ngo, S. S. Chen, N. C. Nguyen, K. L. Tung, *Bioresour. Technol.* **2014**, *160*, 57.

[24] S. I. Mussatto, G. Dragone, I. C. Roberto, *J. Cereal Sci.* **2006**, *43*, 1.

[25] K. Vanreppelen, S. Vanderheyden, T. Kuppens, S. Schreurs, J. Yperman, R. Carleer, *Waste Manag. Res.* **2014**, *32*, 634.

[26] V. Jaikumar, V. Ramamurthi, *Int. J. Chem. (Toronto, ON, Can.)* **2009**,*1*, 1.

[27] J. P. Silva, S. Sousa, I. Gonçalves, J. J. Porter, S. Ferreira-Dias, *Sep. Purif. Technol.* **2004**, *40*, 163.

[28] E. Contreras, L. Sepúlveda, C. Palma, *Int. J. Chem. Eng*. **2012**, *2012*, article ID 679352, 9 pp.

[29] A. Kezerle, N. Velić, H. Pavlović, D. Velić, D. Hasenay, D. Kovačević in *Proceedings Natural resources, green technology & sustainable development 2*, (Eds.: I. Radojčić Redovniković, V. Gaurina Srček, K. Radošević, T. Jakovljević, R. Stojaković, D. Erdec Hendrih), Faculty of Food Technology and Biotechnology University of Zagreb, Zagreb, **2016**, pp. 95–99.

[30] S. T. Ramesh, R. Gandhimathi, T. E. Elavarasi, R. Isai Thamizh, K. Sowmya, P. V. Nidheesh, *Glob Nest J.* **2014**, *16*, 146.

[31] P. R. Ginimuge, S. D. Jyothi, *J. Anaesth. Clin. Pharmacol.* **2010**, *26*, 517.

[32] O. Hamdaoui, M. Chiha, *Acta Chim. Slov.* **2007**, *54*, 407.

[33] A. Afkhami, R. Moosavi *J. Hazard. Mater*. **2010**, *174*, 398.

[34] N. Velić, M. Tišma, I. Jozić, B. Zelić, R. Sudar, S. Keleković, A. Domaćinović in *Proceedings 14th Ružička days "Today science - tomorrow industry"* (Ed.: A. Jukić), Croatian Society of Chemical Engineers, J.J. Strossmayer University of Osijek, Faculty of Food Technology Osijek, Zagreb and Osijek, **2013**, pp. 187–192.

[35] TAPPI, Acid-soluble lignin in wood and pulp. Useful method 246 TAPPI. Atlanta, 1985.

[36] D. B. Rivers, B. R. Zoldak, R. S. Evans, G. H. Emert, *Biotechnol. Lett.* **1983**, *5*, 777.

[37] J. A. Robertson, K. J. A. l'Anson, J. Treimo, C. B. Faulds, T. F. Brocklehurst, V. G. H. Eijsink, K.W. Waldron, *LWT - Food Sci. Technol.* **2010**, *43*, 890.

[38] B. H. Hameed, *J. Hazard. Mater*. **2009**, *162*, 344.

[39] S. D. Khattri, M. K. Singh, *Water, Air, Soil Pollut*. **2000**, *120*, 283.

[40] W. C. Wanyonyi, J. M. Onyari, P. M. Shiundu, *Energy Procedia*. **2014**, *50*, 862.

[41] C. Namasivayam, N. Kanchana, *Pertanika J. Sci. Technol*. **1993**, *1*, 33

[42] M. H. Baek, C. O. Ijagbemi, S. J. O, D. S. Kim, *J. Hazard. Mater.* **2010**, *176*, 820.

[43] R. Abu-El-Halawa, S. A. Zabin, H. H. Abu-Sittah, *Am. J. Environ. Sci.* **2016**, *12*, 213.
[44] O. Hamdaoui, *J. Hazard. Mater.* **2006**, *135*, 264.
[45] T. Yan, L. Wang, *BioResources*. **2013**, *8*, 4722.
[46] D. Suteu, T. Malutan, *BioResources*. **2013**, *8*, 427.
[47] Z. Hu, H. Chen, F. Ji, S. Yuan, *J. Hazard. Mater.* **2010**, *173*, 292.
[48] H.-X. Li, R.-J. Zhang, L. Tang, J.-H. Zhanng, Z.-G. Mao, *BioResources*. **2014**, *9*, 6682.
[49] K. S. Bharathi, S. T. Ramesh, *Appl. Water Sci.* **2013**, *3*, 773.
[50] I. Langmuir, *J. Am. Chem. Soc*. **1918**, *40*, 1361.
[51] H. M. F. Freundlich, *J. Phys. Chem.* **1906**, *57*, 385.
[52] S. Lagergren, K. Svenska, *Vetenskapsad Handl.* **1898**, *24*, 1.
[53] Y. S. Ho, G. McKay, *Chem. Eng. J.* **1998**, *70*, 115.
[54] A. Juhász, E. Csapó, D. Ungor, G. K. Tóth, L. Vécsei, I. Dékány, *J. Phys. Chem. B* **2016**,120, 7844.
[55] R. M. Ali, H. A. Hamad, M. M. Hussein, G. F. Malash, *Ecol. Eng*. **2016**, 91, 317.
[56] S. Pap, J. Radonić, S. Trifunović, D. Adamović, I. Mihajlović, M. Vojinović Miloradov, M. Turk Sekulić, *J. Environ. Manage.* **2016**, *184*, 297.
[57] A. T. Ojedokun, O. S. Bello, *Appl. Water Sci.* **2017**, *7*, 1965.
[58] W. J. Weber, J. C. Morris in *Proceedings of the International Conference on water Pollution Symposium 2*. Pergamon, Oxford, **1962**, pp. 231–266.
[59] W. H. Cheung, Y. S. Szeto, G. McKay, *Bioresour. Technol.* **2007**, *98*, 2897.